Analytical investigation of double negative material based photonic filter performance at 1550 nm

PAMPA DEBNATH[a], ARPAN DEYASI[a,*], UJJWAL MONDAL[b], ANGSUMAN SARKAR[c]
[a]*Department of Electronics and Communication Engineering, RCC Institute of Information Technology, Kolkata, 700015, India*
[b]*Department of Applied Physics, University of Calcutta, Kolkata, 70009, India*
[c]*Department of Electronics and Communication Engineering, Kalyani Govt Engineering College, Kalyani, 741235, India*

Bandwidth in wavelength scale and ripple in passband region of Double Negative (DNG) material based photonic filter is analytically computed at 1550 nm. Transfer matrix technique is adopted for transmittivity computation after evaluating the band structure by Finite Domain Time Difference (FDTD) approach, and two different types of metamaterial, paired nanorod and nano-fishnet with elliptical void are considered for simulation. By suitably choosing the dimensions of constituent materials, passband ripple obtained is minutely small. Results show superiority with those similar filters even at polarized incidence of electromagnetic wave with continuous passband region. Results are important for incorporating the filter as frequency-selective-surface as well as utilizing in all-optical-integrated-circuit.

(Received August 27, 2020; accepted August 16, 2021)

Keywords: DNG material, Photonic filter, Bandwidth, Ripple, Transmissivity

1. Introduction

Ever since the conceptual formation of all-optical integrated circuit [1-2], requirement of photonic components is emerging day-by-day in order to replace the existing electronic counterparts [3] for better SNR, reliability, efficiency or compatible integration with silicon-based devices [4] for scalability and need of high-performance computing. This eventually leads to search of novel materials [5-6] from performance improvement point-of-view, or for different scalable design methodologies with major focus on interconnect [7]. Here comes the importance of photonic crystal, which makes a major breakthrough for design of photonic integrated circuits by enabling the possible realization of different digital [8-9] gates and optical components [10-11]. Several known materials are already used in this purpose [12-13] considering the inherent feature of photonic crystal (PhC) of restricting electromagnetic wave of a few selected wavelengths and allowing others in the direction of propagation; and negative refractive index based materials are the new class added to enhance the selective feature for ultra-narrowband spectrum [14]. These materials, also classified as metamaterials, have not been researched to a good extent for PhC based devices, though extensively analyzed for antenna design [15-16] and also for frequency-selective-surface [17].

Metamaterial based microstrip filter of OLR and SSR types are proposed [18] for antenna applications where geometrical parameter variations are investigated. DNG material based dual bandpass filter is proposed [19] for WLAN and WiMAX applications. Defected ground structure based wideband filter is designed [20] with significantly low insertion loss at the desired region. Filter is also designed with higher transmission peak and very low rejection ratio [21] at THz range, which is applicable for only normal incidence. Filters are also designed at visible and near infrared regions [22] with high emissivity for thermo-photovoltaics applications. Dual band filters are designed [23] with very good stop-band performance. Low-loss filters are proposed [24] using fishnet structures. 2D PhC based tunable filters are recently proposed [25] for WDM applications. However, most of the recent works as available in reputed literatures [26-28] are based on the positive refractive index-based materials, limited number of works are published with DNG materials [29-30] with continuous passband characteristics.

In the present paper, metamaterial based bandpass filter is designed at optical communication wavelength with continuous passband characteristics, where amount of ripple in the desired region is very low. Also the rise and fall of the spectrum is very sharp which makes it suitable as near-ideal optical filter, far better than the designs available in existing literatures. Two different metamaterial structures, namely paired nanorod and nano-fishnet with elliptical void are considered for simulation purpose, and mathematical formulation is established from FDTD approach. Simulated findings are critical for design of pure photonic filter as constituent of all-optical integrated circuits.

2. Mathematical formulation

For computation of photonic bandgap, we first analyze the band structure by finite-difference-time-domain approach, and then bandgap is evaluated. It is then verified by transfer matrix technique for calculation of transmittivity, and corresponding filter profile is plotted around the central wavelength.

Maxwell's equations in a conducting, homogeneous and isotropic medium are given by

$$\frac{\partial \vec{E}}{\partial t} = \frac{1}{\mu\varepsilon}\left[\vec{\nabla}\times\vec{B}\right] - \frac{\sigma}{\varepsilon}\vec{E} \tag{1.1}$$

$$\frac{\partial \vec{B}}{\partial t} = -\left[\vec{\nabla}\times\vec{E}\right] \tag{1.2}$$

Introducing central-difference scheme, we can re-write the equations

$$\frac{E_x^{\,i+1/2}(k) - E_x^{\,i-1/2}(k)}{\Delta t} = -\frac{1}{\mu\varepsilon}\frac{B_y^{\,i}(k+0.5) - B_j^{\,i}(k-0.5)}{\Delta z} \tag{2.1}$$

$$\frac{B_y^{\,i+1/2}(k+0.5) - B_y^{\,i-1/2}(k+0.5)}{\Delta t} = -\frac{1}{\mu}\frac{E_x^{\,i+1/2}(k+0.5) - E_x^{\,i+1/2}(k-0.5)}{\Delta z} \tag{2.2}$$

Since electromagnetic waves of this form are generally polarized, so Bloch conditions are required to compute the complex propagation characteristics.

Results give the existence of electromagnetic bandgap in the band structure profile, and thus transmission profile is obtained.

For applicability of transfer matrix technique (TMT), we first consider TM mode of polarization which may be represented in the following form

$$\vec{\nabla}^2\vec{H}(\vec{r}) + k_0^{\,2}\varepsilon(\vec{r})\vec{H}(\vec{r}) = \vec{0} \tag{3.1}$$

which may be represented in FD form as

$$\frac{H_y^{\,i+1}(k) - 2H_y(k) + H_y^{\,i-1}(k)}{(\Delta y)^2} + k_0^{\,2}\varepsilon(y)H_y(k) = 0 \tag{3.2}$$

Solution of Eq. (3.2) for any arbitrary j[th] layer is given by

$$H_j(y) = a_j \exp{-[ik_j z]} + b_j \exp[-ik_j z] \tag{4}$$

Transfer matrix between two consecutive layers provides phase shift, represented in the form

$$\Phi_{j,j+1} = \begin{pmatrix} \exp[ik_{j,j+1}d_{j,j+1}] & 0 \\ 0 & -\exp[ik_{j,j+1}d_{j,j+1}] \end{pmatrix} \tag{5}$$

Invoking boundary condition at the interface gives

$$\begin{pmatrix} a_{j+1} \\ b_{j+1} \end{pmatrix} = \Lambda_j^{\,j+1}\begin{pmatrix} a_j \\ b_j \end{pmatrix} \tag{6}$$

where

$$\Lambda_j^{\,j+1} = 0.5\begin{pmatrix} 1+\frac{k_{x,j}}{k_{x,j+1}} & 1-\frac{k_{x,j}}{k_{x,j+1}} \\ 1-\frac{k_{x,j}}{k_{x,j+1}} & 1+\frac{k_{x,j}}{k_{x,j+1}} \end{pmatrix} \tag{7}$$

Transmission matrix is defined as the product of the interface matrix with phase

$$T_j^{\,j+1} = \Lambda_j^{\,j+1}\Phi_j^{\,j+1} \tag{8}$$

For a periodic medium following Bragg's law composed of N no of elementary cells, total transmission matrix is given by

$$T^N = T_1^2 T_2^3 \ldots T_{j-1}^{\,j} T_j^{\,j+1} \ldots T_{N-1}^{\,N} \tag{9}$$

Final transmission coefficient is obtained as

$$T(E) = \frac{1}{T_{11}^{\,2}} \tag{10}$$

3. Design and simulation

In this section, we have briefly outlined the FDTD method adopted here for solving the Maxwell's equation. This is a standard procedure, a s earlier adopted by researchers following the preliminary work of Sullivan. For FDTD analysis, we have considered cell size of 1 nm, as the dimension of the structure is at the order of micron. This provides 1000 times' larger structure than the cell size, and naturally the convergence condition is satisfied. The boundary conditions are the absorbing boundary conditions, as mentioned by Sullivan, and for both the field equations respectively, i.e. for Eq. (2.2) and Eq. (3.2) are

$$E_x = E_0 \exp(-jk_x x) \tag{11.1}$$

$$H_y = H_0 \exp(-jk_y y) \qquad (11.2)$$

4. Results and discussion

Based on the mathematical formulation, we first compute the band diagram for the EBG structure considering TM mode of propagation, as depicted in Fig 1. Photonic bandgap is highlighted which speaks that in that region, all the incident wavelengths are reflected. From the plot, it may be concluded that the portions with black color, denotes the stopbands of the filter, whereas rest of the region is passband. This is a normalized plot simulated for paired nanorod structure (n=-0.3), and corresponding transmittivity profile is represented in Fig 2.

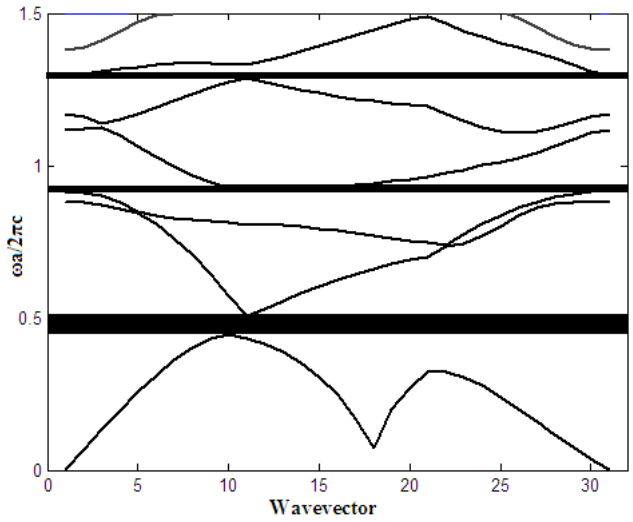

Fig. 1. Band diagram for EBG constituted bypaired nanorod

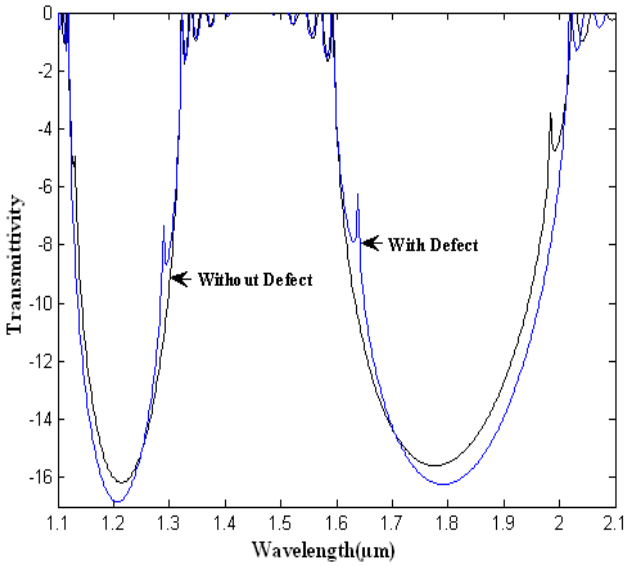

Fig. 2.Transmittivity with wavelength for oblique incidence of TM mode in presence and absence of defect (color online)

From the plot, it is found that with suitable choice of layer width, ripple in the passband can be made negligibly small, as evident from the plot. Also result is compared with the defected structure, where sharp natures of passband sidewalls are little deviated. Here percentage of defect is considered within tolerable range (3% line defect) so that the device can work efficiently as filter. Similar results for elliptical void structure are already reported [31], precisely for TE mode [32].

Transmissivity in TM mode is also calculated for different dimensions of the materials as well as different angle of incidence. Results are represented in Figs 3.1-3.3From Fig. 3.1, it is seen that transmittance is decreased at the notches in the range 1.1 μm-1.3 μm and is also decreased at 1.6 μm-2.0 μm when propagation length of metamaterial layer is increased, which reveals the fact that suitable introduction of propagation length in alternative single layer enhances the filter characteristics. It may also be noted that ripple is reduced in passband. Comparing the plot with already published data for TE mode [32], we find that width of notch (in wavelength scale) is higher for TM wave which reduces width of passband, i.e., narrow bandpass filter is obtained. Length of notch (in transmittance scale) is higher for TM wave which speaks about better passband characteristics. Also change of air-thickness modulates both ripple and passband width, as evident from Fig 3.2.

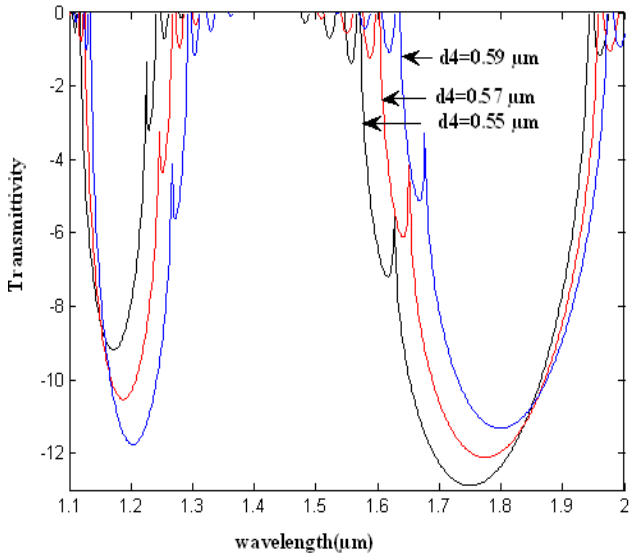

Fig. 3.1.Transmittivity with wavelength for oblique incidence (7°) of TE mode in presence of defect for differentpropagation length ofair thickness for paired nanorod (color online)

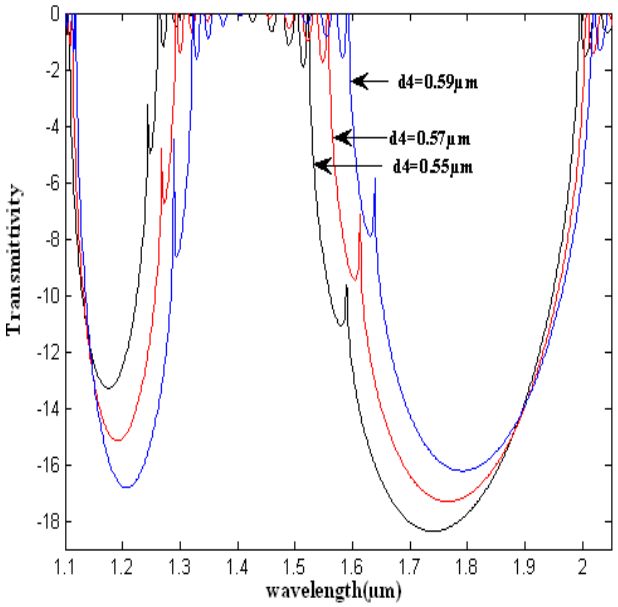

Fig 3.2. Transmittivity with wavelength for oblique incidence (7°) of TM mode in presence of defect for different length of airnano-fishnet with elliptical void (color online)

From Fig 3.3, it is seen that with increase of incident angle, width in the passband region slowly increases, along with generation of unwanted ripple in passband. However, width is narrower as compared with that obtained for TE mode. Similar variations are observed for nano-fishnet with elliptical void structure [31].

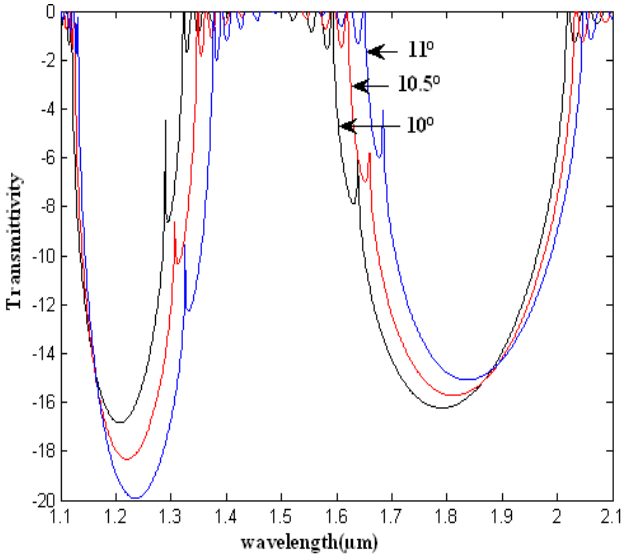

Fig 3.3. Transmittivity with wavelength for oblique incidence of TM mode in presence of defect for different incident anglefor paired nanorod (color online)

In Table 1 and Table 2, we have made a comparative study with the data obtained for different photonic filter structures designed at different communication wavelengths. Results are compared with the proposed structure in terms of bandwidth, ripple and maximum transmittivity. All the computations are taken from the transmittivity profile. Table 1 deals with metal-dielectric structures, whereas Table 2 consists of dielectric-dielectric structures.

From the dataset, we may conclude that the proposed structure provides maximum transmittivity which is desired for any filter structure, and simultaneously minimum ripple in the narrow passband region. This optimum performance is yet to be achieved by the metal-dielectric PhC structures as published in different literatures. The bandwidth for the various structures as reported are wider compared to our result which accounts for higher ripple in either side of passband. Thus SNR is reduced with the additional factor that in all the reported results, maximum transmittivity is less than the desired value; which accounts for further detoriation in filter performance. Similar comparative study is performed with dielectric-dielectric structures, as shown in Table 2. In both the sets, comparison is made for normal and all types of polarized incidences.

In Table 3, defected structures are considered as it is more practical compared with the ideal structure, and comparison is carried out. Results are only computed for normalized incidence, and are compared with both the metamaterial based structures. Significant improvement is seenfor all the cases.

Table 1. Comparative study of filter performance for MPC structures

Material	Type of incidence	Maximum transmittivity	Bandwidth [nm]	Average ripplein passband [normal-ized scale]
Ag-SiO_2 [33]	p-polarization (50°)	0.9	275	0.15
Ag-SiO_2 [33]	s-polarization (50°)	0.75	250	0.2
Au-SiO_2 [33]	p-polarization (50°)	0.7	325	0.02
Au-SiO_2 [33]	s-polarization (50°)	0.6	275	0.08
Cu-SiO_2 [33]	p-polarization (50°)	0.45	275	---
Cu-SiO_2 [33]	s-polarization (50°)	0.25	225	---
Li- SiO_2 [33]	p-polarization (50°)	0.75	250	0.02
Li- SiO_2 [33]	s-polarization (50°)	0.6	230	0.05
Cryolite-Silver [34]	normal	0.9	150	0.2
Cryolite-Silver [34]	p-polarization (10°)	0.9	200	0.35
Cryolite-Silver [34]	s-polarization (10°)	0.9	175	0.2
Proposed structure using paired nanorod	normal	1.0	205	0.03
Proposed structure using paired nanorod	p-polarization (50°)	1.0	200	0.02
Proposed structure using paired nanorod	s-polarization (50°)	1.0	198	0.02
Proposed structure using paired nanorod	normal	1.0	200	0.02
Proposed structure using paired nanorod	p-polarization (10°)	1.0	198	0.03
Proposed structure using paired nanorod	s-polarization (10°)	1.0	198	0.02

Table 2. Comparative study of filter performance with DPC structures (without defect)

Material	Type of incidence	Maximum transmittivity	Bandwidth [μm]	Average ripple in passband [normal-ized scale]
Cryolite-Silicon [34]	normal	1.0	400	0.35
Cryolite-Silicon [34]	p-polarization (10°)	1.0	225	0.35
Cryolite-Silicon [34]	s-polarization (10°)	1.0	275	0.35
Si-SiC [35]	normal	1.0	840	0.1
SiO_2-TiO_2 $(AB)_{16}$ [36]	normal	0.9	390	0.15
SiO_2-TiO_2 $(ABBA)_8$ [36]	normal	0.8	200	0.15
SiO_2-TiO_2 $(ABBABAAB)_4$ [36]	normal	0.8	375	0.2
Proposed structure using paired nanorod	normal	1.0	200	0.02
Proposed structure using paired nanorod	p-polarization (10°)	1.0	198	0.03
Proposed structure using paired nanorod	s-polarization (10°)	1.0	198	0.02

Table 3. Comparative study of filter performance with DPC structures (with defect)

Material	Type of incidence	Maximum transmittivity	Bandwidth [nm]	Average ripple in passband [normalized scale]
SiO_2-TiO_2 $(AB)_{16}$ [36]	normal	0.9	500	0.1
SiO_2-TiO_2 $(ABBA)_8$ [36]	normal	0.9	400	0.15
SiO_2-TiO_2 $(ABBABAAB)_4$ [36]	normal	0.9	425	0.15
Proposed structure using paired nanorod	normal	1.0	200	0.03
Proposed structure using nano-fishnet with elliptical void	normal	1.0	195	0.03

Next bandwidth of the proposed structures is computed form transmittivity profile, and results are graphically represented in Figs. 4.1-4.2 Various structural as well as external parameters are tailored within experimentally realizable range,and continuous profile is obtained though monotonous change is not achievable for all the cases.

The critical factor in designing a PhC based filter is the determination of performance for various angle of incidence, as it is that external factor which is beyond the control of tuning when the component is embedded in all-optical circuit. However, care is always taken so that the deviation should be as less as possible. In Fig. 4.1, results are plotted for different lengths of the structure at 7° angle of incidence for nano-fishnet structure, whereas in Fig. 4.2 the same is computed for paired nanorod. A brief comparison shows that tailoring of the gap (air thickness) in the structure makes a smooth monotonous variation of bandwidth, whereas random fluctuation is observed when length of the material is changed. This is due to the fact that widening the gap does not disturb the E-field or H-field, whereas these are directly associated with the structure is concerned.

For void geometry, bandwidth is also computed for three different angles of incidence, and represented in Fig.5. Shape of the ellipse is tailored at different angle, and corresponding bandwidth is measured around 1550 nm. For 7° angle, result is already shown in Fig 4.1. We have further simulated for 10° angles. By keeping the structure constant, bandwidth is also measured with respect to change of incidence angle within practical limit. This is plotted in Fig. 6.

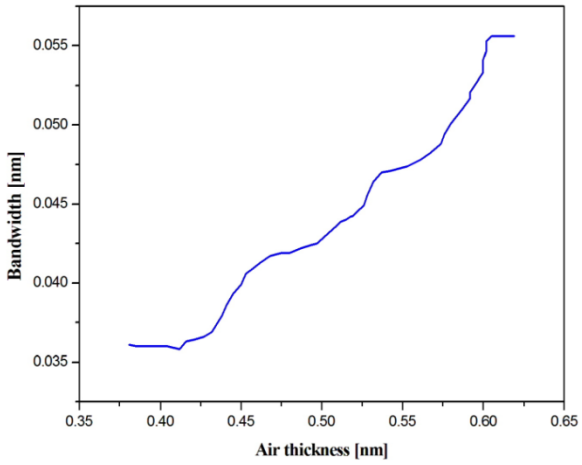

(a)

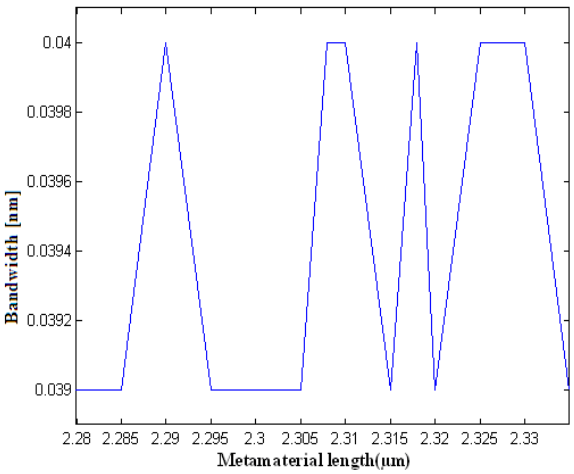

(b)

Fig 4.1. Bandwidth with length of the structure for nano-fishnet structure at 7° angle of incidence (a) for different air thickness; (b) for different length of metamaterial (color online)

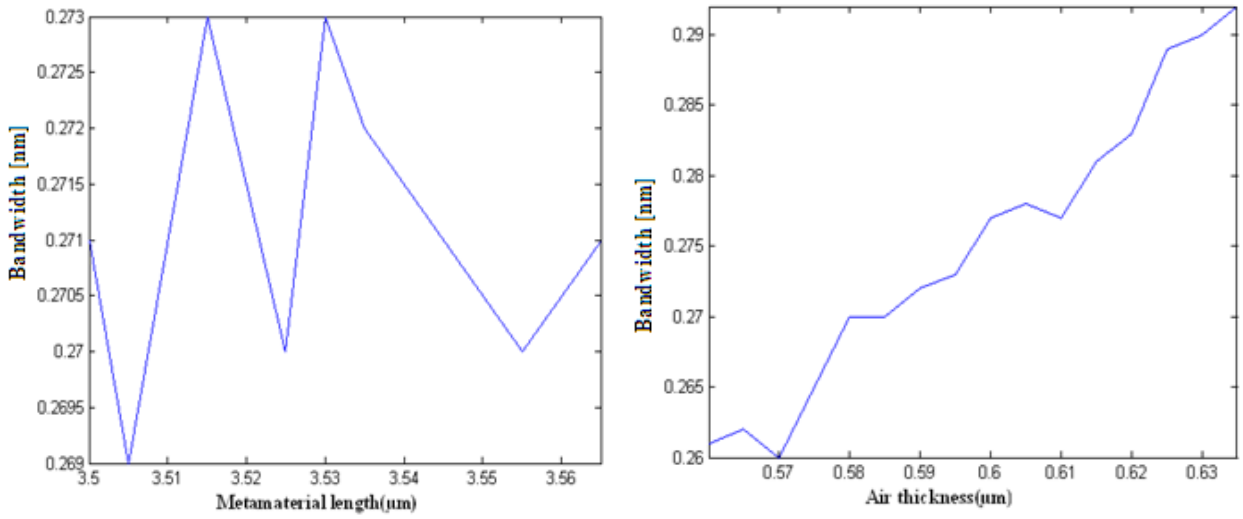

(a) *(b)*

Fig 4.2. Bandwidth with length of the structure for paired nanorod at 7° angle of incidence (a) for different air thickness; (b) for different length of metamaterial (color online)

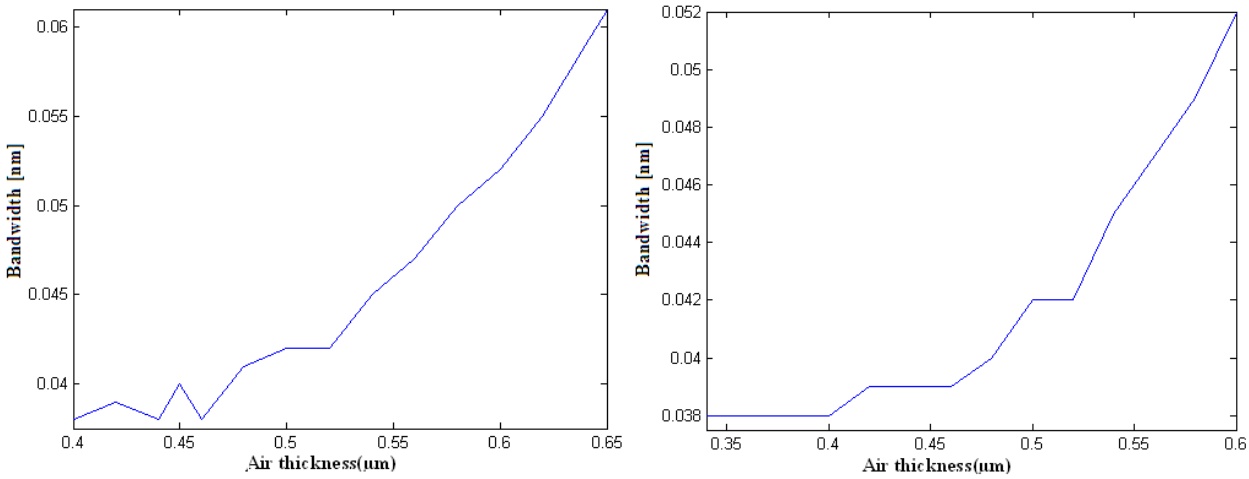

(a) *(b)*

Fig.5. Bandwidth with length of the structure for nano-fishnet structure at (a) 7° angle of incidence (b) 10° angle of incidence

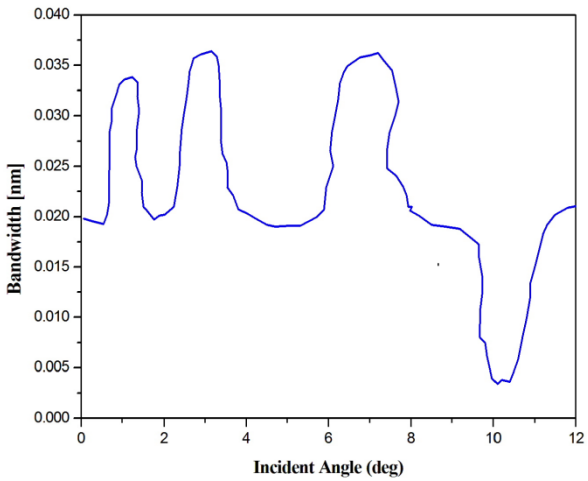

Fig.6. Bandwidth with wavelength for TM mode in presence of defect for different incident angle (color online)

5. Conclusion

Simulated findings shows that metamaterial structure provides better performance as filter at 1550 nm when compared with the filters constituted by materials with positive refractive indices. Higher transmittance is observed at passband region compared with the other structures with minimum ripple in passband, and sharp transition regions. Also suitable choice of material dimension makes it a narrow passband filter which effectively helps to enhance signal-to-noise ratio. In order to take into realistic design, presence of point defects is considered for computation purpose. Variation of angle of incidence is taken care to observe the practical range of bandwidth when implemented in all-optical integrated circuit.

References

[1] G. Roelkens, Frontiers in Optics: OSA Technical Digest,FF5F.4 (2016).

[2] F. Kish, V. Lal, P. Evans, S. W. Corzine, M. Ziari, T. Butrie, M. Reffle, H.-S. Tsai, A. Dentai, J. Pleumeekers, M. Missey, M. Fisher, S. Murthy, R. Salvatore, P. Samra, S. Demars, N. Kim, A. James, A. Hosseini, P. Studenkov, M. Lauermann, R. Going, M. Lu, J. Zhang, J. Tang, J. Bostak, T. Vallaitis, M. Kuntz, D. Pavinski, A. Karanicolas, B. Behnia, D. Engel, O. Khayam, N. Modi, M. R. Chitgarha, P. Mertz, W. Ko, R. Maher, J. Osenbach, J. T. Rahn, H. Sun, K.-T Wu, M. Mitchell, D. Welch, IEEE Journal of Selected Topics in Quantum Electronics **24**(1), 6100120 (2018).

[3] R. S. Tucker,Journal of Lightwave Technology **24**(12), 4655 (2006).

[4] A. H.Atabaki,Nature **556**, 349 (2018).

[5] M. Lipson, 74th Annual Device Research Conference, 2016.

[6] Q.Wu, J. P. Turpin, D. H. Werner, Light: Science & Applications **1**, e38 (2012).

[7] A. Farsaei, J. Klein, J. Pond, J. Flueckiger, X. Wang, G. Lamant, L. Chrostowski, S. Mirabbasi, Advanced Photonics: OSA Technical Digest, JTu4A.2, 2016.

[8] S. N. Achary, Journal of Material Sciences & Engineering **4**(4), 1000178 (2015)

[9] K. Bhadel, R. Mehra, International Conference on Computational Intelligence and Communication Networks, 2014.

[10] W. Tong, J. Wang, T. Qiu, Z. Liu, W. Wang, S. Qu, Progress in Electromagnetic Research Symposium, 2016.

[11] S. Singh, K. Singh, Optik **145**, 495 (2017).

[12] X. Zhao, Y. Yang, Z. Chen, Y. Wang, H. Fei, X. Deng, Journal of Semiconductors **38**(2), 023004 (2017).

[13] S. Saravi, T. Pertsch, F. Setzpfandt, Conference on Lasers and Electro-Optics: OSA Technical Digest, FTh1G.2, 2018.

[14] J. Čtyroký, J. G. Wangüemert-Pérez, P. Kwiecien, I. Richter, J. Litvik, J. H. Schmid, I. Molina-Fernández, A. Ortega-Moñux, M. Dado, P. Cheben, Optics Express **26**, 179 (2018).

[15] H. Kumar, R. K. Kanth, P. Liljeberg, H. Tenhunen, 10thInternational Conference on Telecommunication in Modern Satellite Cable and Broadcasting Services, 2011.

[16] T. A.Elwi, B. A. Ahmad, AEU - International Journal of Electronics and Communications **96**, 122 (2018).

[17] A. Yelizarov, A. Kukharenko, German Microwave Conference, 2016.

[18] K. C. Jayakrishnan, N. S. Bhuvana, K. M. Sreedevi, 3rd International Conference on Signal Processing and Integrated Networks, 2016.

[19] A. K. Gorur, C. Karpuz, A. Ozek, M. Emur, Microwave and Optical Technology Letters **56**(10), 2211 (2014).

[20] S.Chaimool, P. Akkaraekthalin, Radioengineering **21**(2), 611 (2012).

[21] O. Paul, R. Beigang, M. Rahm, Optics Express **17**(21), 18590 (2009).

[22] J. B. Brückner, J. L. Rouzo, L. Escoubas, G. Berginc, O. Calvo-Perez, N. Vukadinovic, F. Flory, Optics Express **21**, 16992 (2013).

[23] W. Junlin, Z. Binzhen, W. Xin, D. Junping, Optical Material Express **7**, 1656 (2017).

[24] L. Lin, Z. H. Jiang, S. Yun, D. H. Werner, T. S. Mayer,Proc of SPIE: Advanced Fabrication Technologies for Micro/Nano Optics and Photonics **8974**, 897410 (2014).

[25] G. Moloudian, R. Sabbaghi-Nadooshan, M. Hassangholizadeh-Kashtiban, Journal of the Chinese Institute of Engineers **39**(8), pp. 971 (2016).

[26] S. Robinson, AIP Conference Proceedings **1620**, 131 (2014).

[27] P. A. Islam, N. Sultan, S. Nayeem, B. Bhuian, IEEE Region 10 Symposium, 2014.

[28] G. Rajalakshmi, A. S. Raja, D. S. Sundar, Journal of Nonlinear Optical Physics & Materials **24**(3), 1550027 (2015).

[29] Y. Zhao, B. Jiang, B. Li, D. Wang, Optoelectronics Letters **12**(4), 273 (2016).

[30] Y. T. Jin, L. M. Si, Q. L. Zhang, J. Q. Feng, X. Lv, IEEE 6th International Symposium on Microwave, Antenna, Propagation, and EMC Technologies, 2015.

[31] S. Ghosh, R. Dutta, V. Shaw, A. Deyasi, Springer Proceedings in Physics: Advances in Optical Science and Engineering, ch.**62**, 507 (2017).

[32] A. Deyasi, S. Ghosh, R. Dutta, V. Shaw, Comparative Analysis of Filter Performance in DNG Material based Photonic Crystal Structure, CRC Press: Advancement of Computer Communication and Information Technology, 181 (2016).

[33] A. H. Aly, Wave propagation in materials for modern applications, Ed: Petrin A, Intech, 193 (2010).

[34] A. H. Aly, M. Ismaeel, E. Abdel-Rahman, Optics and Photonics Journal **2**, 105 (2012).

[35] A. Chakraborty, IOSR Journal of Electronic and Communication engineering **5**(6), 34 (2013).

[36] A. Petcu, L. Preda, Romanian Journal of Physics **54**(5-6), 539 (2009).

*Corresponding author: deyasi_arpan@yahoo.co.in